DOI: 10.1002/chem.200801776

Zr–Zeolite Beta: A New Heterogeneous Catalyst System for the Highly Selective Cascade Transformation of Citral to (±)-Menthol

Yuntong Nie, Stephan Jaenicke, and Gaik-Khuan Chuah*[a]

Abstract: The transformation of citral to menthols involves hydrogenation steps as well as cyclisation of the intermediate, citronellal. The ability of Zr–zeolite beta to catalyse the cyclisation with high diastereoselectivity to (±)-isopulegol is the critical step in this cascade transformation. Bifunctional catalysts containing nickel or rhodium supported on Zr–zeolite beta gave menthols in yields of 87–89% and an excellent diastereoselectivity of 94% for the desired (±)-menthol. Dual catalyst systems of Zr–zeolite beta and nano-dispersed Ni on an MCM-41 support were equally effective and have the added advantage that the rates of the acid- and hydrogenation-catalysed steps can be independently varied. By applying a pressure ramp of 0.2–2 MPa, the yield of menthols could be increased to 95%, with 94% diastereoselectivity for (±)-menthol. The low initial pressure minimises the rates of competing hydrogenation reactions to byproducts such as citronellol and 3,7-dimethyloctanol.

Keywords: cyclization · heterogeneous catalysis · hydrogenation · zeolites · zirconia

Introduction

Catalytic cascade conversions are increasingly considered for organic syntheses due to savings in time, energy and materials.[1] Such conversions eliminate the recovery of intermediates and the presence of a catalyst minimises the need for stoichiometric amounts of reagents, thereby reducing the waste generated. The one-pot transformation of 3,7-dimethyl-2,6-octadienal (citral) to menthols involves a triple cascade of hydrogenation, isomerisation and hydrogenation steps (Scheme 1). The first step in this route requires a highly selective route in which the conjugated C=C bond in citral is first hydrogenated to form (±)-citronellal (**2**). The choice of metal catalyst affects the adsorption and reaction of citral, and can result in different product distributions **2**–**8**.[2] Palladium, nickel and rhodium show good selectivity towards hydrogenation of the conjugated C=C bond rather than the C=O group, thus giving **2** in high yield.[3] Theoretical calculations by Delbecq and Sautet[4] showed that this selectivity can be explained in terms of a narrow d band,

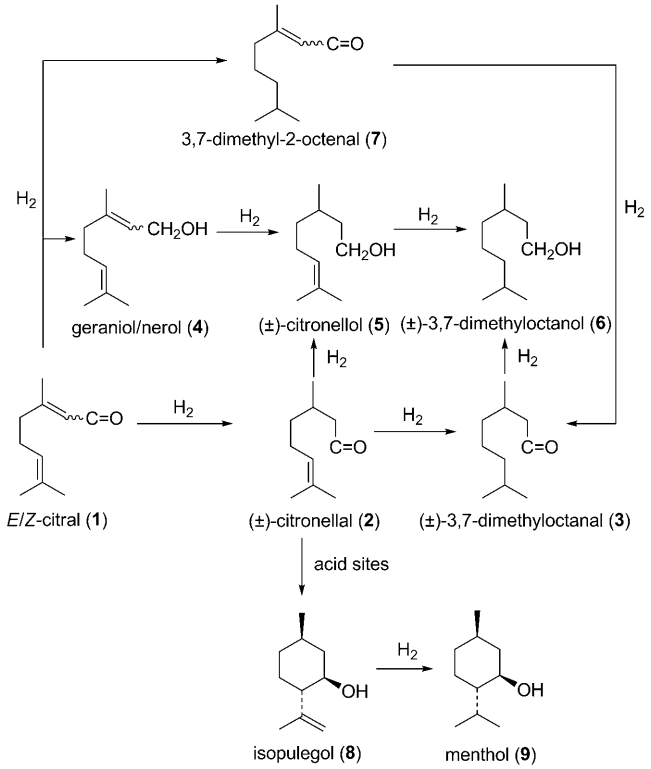

Scheme 1. Reaction products in the hydrogenation of citral.

[a] Dr. Y. Nie, Prof. S. Jaenicke, Prof. G.-K. Chuah
Department of Chemistry, National University of Singapore
3 Science Drive 3, Kent Ridge, Singapore 117543
Fax: (+65) 6516-2839
E-mail: chmcgk@nus.edu.sg

Supporting information for this article is available on the WWW under http://dx.doi.org/10.1002/chem.200801776.

which reduces the destabilising four-electron interactions and allows for greater interaction between the conjugated C=C bond and the metal surface. The selectivity is altered by the addition of $FeCl_2$, which activates the C=O bond for hydrogenation. Under these conditions, about 30% of the reaction products were unsaturated alcohols, geraniol and nerol (**4**).[5]

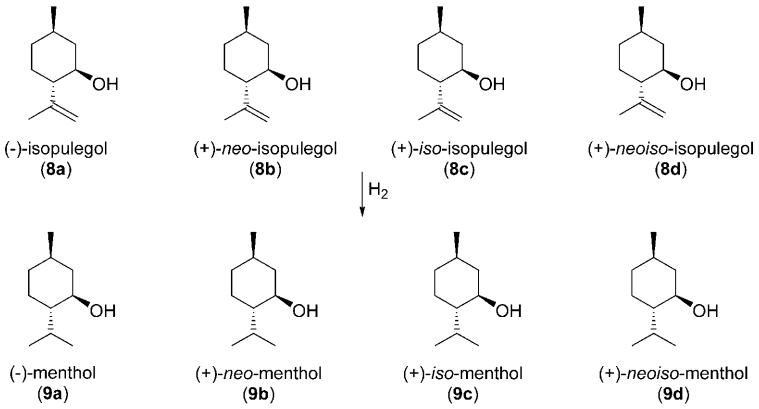

The choice of the support and reaction conditions can also influence the selectivity of the hydrogenation of citral, for example, nickel deposited through atomic layer epitaxy onto alumina gave citronellol (**5**) in around 95% yield.[6] However, nickel supported on activated carbon gave only low citral conversion due to insufficient impregnation of the metal as well as catalyst deactivation.[7] When the nickel catalyst is supported on an alumina-washcoat cordierite monolith, either **2** or 3,7-dimethyloctanol (**6**) can be formed depending on the hydrogen pressure. Lower pressures (0.5 MPa) favour **2**, but a higher pressure of 4 MPa H_2 leads to **6**.[8] By using ionic liquids together with palladium acetylacetonate immobilised on activated carbon cloth, Mikkola et al.[9] found that different hydrogenated products were formed depending on the solubility of hydrogen in the ionic liquid.

Cyclisation of **2** results in isopulegol (**8**). Each diastereoisomer of **8** occurs as a pair of enantiomers: (±)-isopulegol (**8a**), (±)-*neo*-isopulegol (**8b**), (±)-*iso*-isopulegol (**8c**) and (±)-*neoiso*-isopulegol (**8d**). Hydrogenation of **8** leads to four pairs of menthol enantiomers: (±)-menthol (**9a**), (±)-*neo*-menthol (**9b**), (±)-*iso*-menthol (**9c**) and (±)-*neoiso*-menthol (**9d**). The isomer with the highest commercial value is (−)-menthol, which has a peppermint odour and also exerts a physiological cooling effect.[10] The latter property is peculiar to this isomer and none of the other isomers possess this "refreshing" property. Hence, (−)-menthol is widely used in products such as pharmaceuticals, cosmetics, toothpastes, chewing gum and cigarettes. Although most (−)-menthol is obtained from freezing the oil of *Mentha arvensis* to crystallise the menthol, in the year 2007 about 6300 tonnes were prepared by chemical synthesis.[11] In the Takasago process starting from myrcene, the intermediate (+)-**2** is cyclised to **8** over homogeneous zinc bromide as the Lewis acid catalyst.[12] The ratio of (−)-**8** to the other isomers is 94:6. To obtain a high yield of 74.5%, the reaction must be carried out at 110°C. In a recent patent,[13] the diastereoselectivity for (−)-**8** was improved to 99.7:0.3 by using homogeneous tris(2,6-diarylphenoxy)aluminium catalysts. However, workup with sodium hydroxide and separation is necessary to obtain the product.

The use of solid catalysts offers the advantages of ease of separation and recovery of product(s) and catalyst from the reaction medium. However, the diastereoselectivity for (−)-**8** when using Al-zeolite beta, MCM-41, HY, mordenite, Ru-$ZnBr_2/SiO_2$, Cu/SiO_2, and recently, Zr-TUD-1, catalysts is only between 52–76%.[14] We have previously shown that Zr–zeolite beta (Zr-beta) is an active catalyst for the cyclisation of (±)-**2** to **8** with an overall selectivity greater than 98%.[15] The high activity is attributed to a combination of strong Lewis acid sites and weak Brønsted acid sites required for cyclisation. Unique amongst other types of heterogeneous catalysts, Zr-beta catalyses the formation of **8a** with a very high diastereoselectivity of 92–94%, making it comparable with the 94% diastereoselectivity reported for the $ZnBr_2$ catalyst. We postulate that the presence of the bigger Zr^{4+} ion instead of Al^{3+} in the pore channels of Zr-beta restricts the pore accessibility, in turn dictating the selectivity of the isomerisation products. Indeed, studies using X-ray absorption fine structure on Sn-beta shows that Sn occupies specific crystallographic sites in the six-membered rings.[16] These partially hydrolysed framework heteroatoms form the active sites in Sn-beta and Zr-beta.[17] Only the diastereomer **8a** can have all substituents, methyl, hydroxyl and propenyl, in the equatorial positions. The other diastereomers, **8b–d**, have at least one substituent in the axial position. The formation of these isomers is hindered if the pore size is restricted. We have studied nickel supported on Zr-beta for the direct transformation of (±)-**2** to menthols and found that a nickel loading of 4 wt% was optimum in giving a good selectivity for menthols, 96%, with 90% diastereoselectivity for **9a**.[18] The high selectivity for menthols was aided by a delayed introduction of hydrogen, thus favouring the cyclisation of **2** to **8** over the competing hydrogenation reactions to **3**, **5** and **6**. The low nickel loading reflects a balance of hydrogenation and zirconium Lewis acid sites to maximise the selectivity from (±)-**2** to menthols.

In the synthetic production of menthol, the usual starting compounds are cresol, thymol, isoprene, limonene and **2**. The demand for menthol is inelastic, so that very slight variations in supply can result in tremendous price fluctuations.[11,19] A viable synthesis starting from citral widens the choice of raw starting material, although the main use of citral is in the synthesis of vitamin A. The one-pot synthesis

of menthols from citral was first reported by Trasarti et al.[20] using nickel supported on a moderately acidic support, Al-MCM-41. A total yield of menthols of 94% with a selectivity for **9a** of 72.3% was found. Byproducts were due to decarbonylation and cracking. In another study by Mäki-Arvela et al.,[21] H-MCM-41 (Si/Al 20) and HY were compared as supports for nickel. When HY zeolite was used as a support, the strong citral adsorption onto the acidic sites led to severe catalyst deactivation. Mainly hydrogenolysis products were obtained and only a 4% conversion to menthols was observed. Although mesoporous H-MCM-41 was a better support, the yield of menthols at 100% conversion of citral was only 54%, with the remainder being products such as menthatrienes, aromatics and menthadienes. For both supports, the diastereoselectivity for **9a** was between 70 and 75%. To increase the diastereoselectivity for **9a**, we explored the feasibility of using Zr-beta in the cascade transformation of citral to menthols. Zr-beta is used as a support for metal catalysts, nickel, rhodium and palladium, thus forming a bifunctional catalyst with acid and hydrogenation sites. In addition, Zr-beta is used in combination with an MCM-41-supported metal catalyst in a dual catalyst system.

Results and Discussion

Catalyst characterisation: The powder X-ray diffractograms of the metal-impregnated Zr-beta samples exhibited the characteristic peaks of Zr showing that impregnation did not destroy the zeolitic crystalline structure (Figure 1). However, the diffractogram of 15 wt% Ni/Zr-beta-HDP, prepared by deposition–precipitation, additionally showed a broad hump for $2\theta \approx 20$–$40°$, indicative of the presence of some amorphous phase. Reflexes due to nickel could be detected in the X-ray diffractograms for 10 and 15 wt% Ni supported on Zr-beta. By using the Debye–Scherrer equation, the size of the nickel crystallites was calculated to be about 27 and 33 nm, respectively (Table 1). In contrast, no reflexes due to nickel were observed in the diffractogram of 15 wt% Ni/Zr-beta-HDP. This method obviously results in the precipitation of much smaller nickel crystallites below the detection limit of XRD. This was confirmed by TEM micrographs, which showed that the size of the nickel crystallites formed by deposition–precipitation were between 0.5 and 3 nm, whereas those resulting from wet impregnation were larger, 7–28 nm. In addition, Zr-beta appeared to be partially destroyed by the presence of urea during the deposition–precipitation process (Figure 2a). Under the alkaline conditions, delamination of Zr-beta resulted in long thread-like whiskers. Careful analysis revealed that these whiskers were not nickel, but rather layers of silica that had exfoliated and were rolled up in thread-like structures.

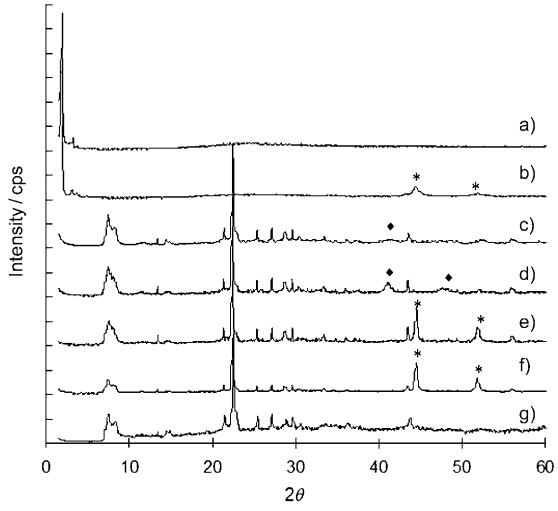

Figure 1. X-ray diffraction patterns of a) 3 wt% Ni/MCM-41, b) 15 wt% Ni/MCM-41, c) 2 wt% Rh/Zr-beta, d) 5 wt% Rh/Zr-beta, e) 10 wt% Ni/Zr-beta, f) 15 wt% Ni/Zr-beta and g) 15 wt% Ni/Zr-beta-HDP. Reflections of metallic nickel are indicated by * and rhodium is indicated by ◆.

Table 1. Textural properties of catalysts.

Sample	S_{BET} [$m^2 g^{-1}$]	S_{micro} [$m^2 g^{-1}$]	V_{total} [$cm^3 g^{-1}$]	V_{micro} [$cm^3 g^{-1}$]	Crystal size[a] [nm]
Zr-beta	476	402	0.25	0.20	–
10% Ni/Zr-beta	431	342	0.24	0.18	27
15% Ni/Zr-beta	404	336	0.24	0.17	33
15% Ni/Zr-beta-HDP	381	224	0.44	0.11	–
0.5% Rh/Zr-beta	473	403	0.26	0.20	–
2% Rh/Zr-beta	443	358	0.26	0.17	13
5% Rh/Zr-beta	352	307	0.22	0.16	15
MCM-41	948	35.4	0.91	0.02	–
3% Ni/MCM-41	947	33.6	0.90	0.02	–
15% Ni/MCM-41	659	39.9	0.69	0.02	8
2% Pd/MCM-41	780	0	0.61	0	–

[a] Calculated from the Debye–Scherrer equation.

The nitrogen adsorption–desorption isotherms of the HDP sample showed a steep rise at $P/P_o \approx 0.45$, corresponding to mesopores about 3.8 nm in diameter (Figure 2b). In comparison, the porous structure of Zr-beta was unchanged by wet impregnation of the same loading of nickel, although there was less adsorption at low P/P_o, which indicates a reduction in the number of micropores.

The acidity of the metal-containing zeolites was determined by IR spectroscopy following the adsorption of pyridine at room temperature and desorption at 100°C (Figure 3). The band at around 1446 cm^{-1} is due to pyridine bonded to Lewis acid sites, whereas the band at 1545 cm^{-1} is assigned to pyridinium ions formed at Brønsted acid sites.[22] Zr-beta has predominantly Lewis acidity with some Brønsted acid sites. Despite nickel loading, the 15 wt% Ni/Zr-beta sample still has both Lewis and Brønsted acidity, with a slight decrease in the density of the latter.

Similar to Ni/Zr-beta, the surface area of Rh/Zr-beta samples prepared by wet impregnation decreased with rhodium loading. This can be attributed to blocking of the micropores by metal crystallites. Despite the low loading, the rhodium phase could be detected in the X-ray diffractograms of the 2

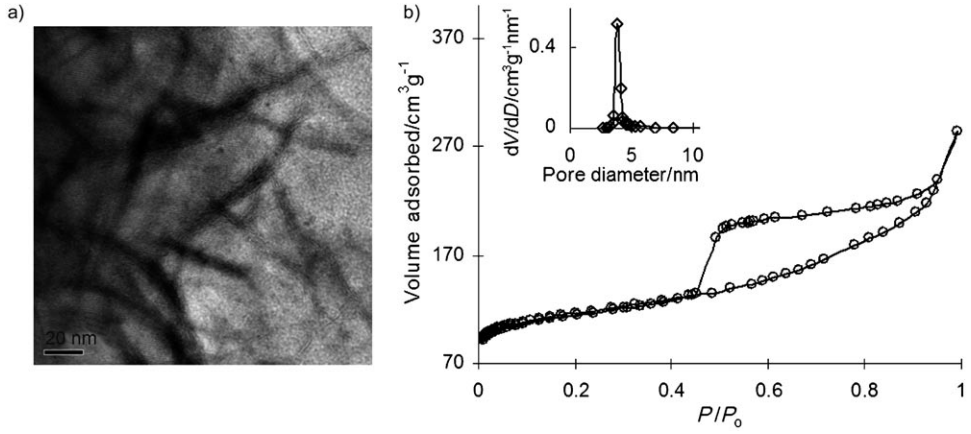

Figure 2. a) TEM image and b) nitrogen adsorption–desorption isotherm of 15 wt% Ni/Zr-beta-HDP. Inset: pore size distribution.

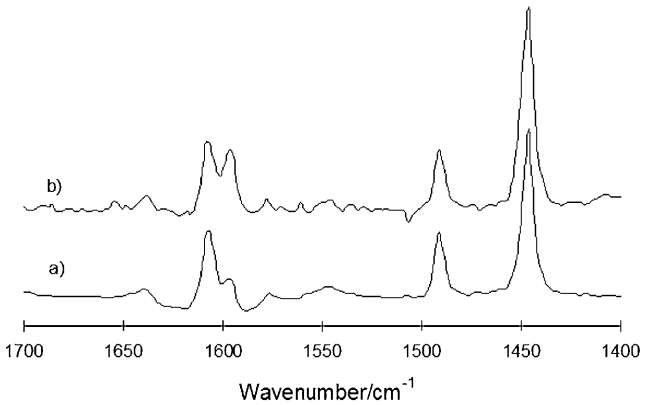

Figure 3. Pyridine IR spectra of a) Zr-beta and b) 15 wt% Ni/Zr-beta.

and 5 wt% Rh/Zr-beta, showing that bigger metal crystallites are formed relative to Ni/Zr-beta (Figure 1).

The surface area of the 3 wt% Ni/MCM-41 was high, 947 m^2g^{-1}, and very similar to that of the pure support (Table 1). However, after loading with 15 wt% Ni, the surface area was reduced to 659 m^2g^{-1}. The powder X-ray diffractograms of the MCM-41-supported samples showed the characteristic (100), (110) and (200) diffraction peaks of the support at low 2θ values (Figure 1). The nickel phase could be clearly observed in the X-ray diffractogram of the 15 wt% Ni/MCM-41. The crystallite size was calculated by the Debye–Scherrer equation to be about 8 nm, which is smaller than those deposited on 15 wt% Ni/Zr-beta.

Bifunctional Ni/Zr-beta catalyst: Preliminary studies using low nickel loadings of 3–5 wt% on Zr-beta resulted in very low reaction rates. Citral was only fully converted after two to three days. Therefore, higher loadings of 10 and 15 wt% were used. For 10 wt% Ni/Zr-beta, the concentration of citral decreased to <5% after 4 h (Figure 4a). Compound (±)-**2** was formed and cyclised to form **8** over 10 h. Of the four isomers, only **8a**, **8b** and **8c** were detected in the ratio of 94:5:1. No **8d** was detected. The rather high concentration of **8** during the course of reaction showed that the hydrogenation to menthols **9a–c** is slow. The initial rate of menthol formation was low and rapidly increased only after 4 h, resulting in a menthol yield of 89% after 22 h. The diastereoselectivity for the desired **9a** was high (94%; Table 2, entry 1). When the nickel loading was increased to 15 wt%, the rate of hydrogenation of citral was very similar to that for 10 wt% Ni/Zr-beta. However, the subsequent hydrogenation of **8** to menthols was faster with

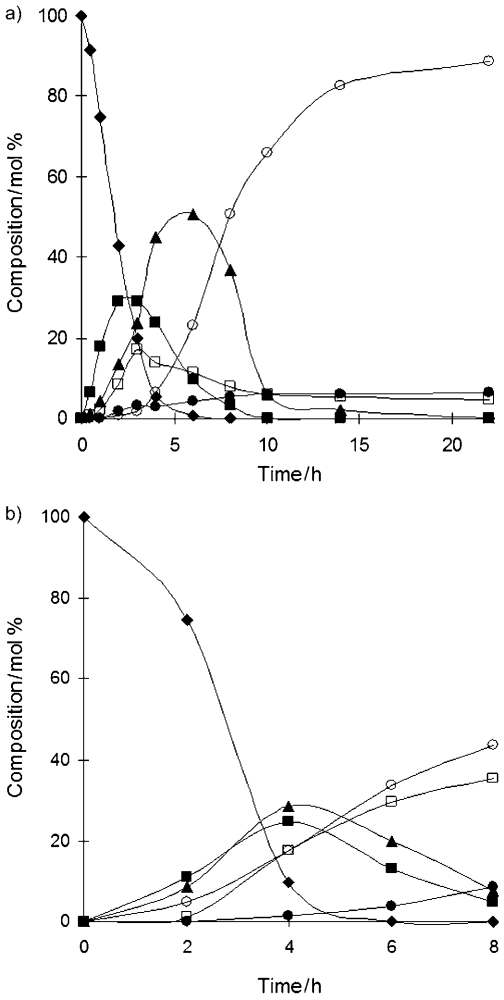

Figure 4. Hydrogenation of citral over a) 10 wt% Ni/Zr-beta and b) 15 wt% Ni/Zr-beta-HDP. (◆) Citral (■) **2** (▲) **8** (○) menthols (□) **5**, and (●) **6**. Reaction conditions: citral (9.9 mmol), *tert*-butanol (50 mL), catalyst (0.15 g), 80 °C, 2 MPa H_2.

Table 2. Hydrogenation of citral over bifunctional Zr-beta catalysts and dual catalytic systems.[a]

	Catalyst	P	*t*	X	Selectivity [%]						Yield [%]
		Mpa	[h]	[%]	**9** (**9a**)	**5**	**6**	**8**	**2**	**3**	**9** (**9a**)
1	10 % Ni/Zr-beta	2	22	100	89 (94)	4	7	0	0	0	89 (84)
2	15 % Ni/Zr-beta	2	22	100	87 (92)	4	7	1	0	0	87 (80)
3	15 % Ni/Zr-beta-HDP	2	8	100	44 (78)	35	9	8	5	0	44 (34)
4	0.5 % Rh/Zr-beta	2	24	65	2 (100)	4	9	81	4	0	2 (2)
5	2 % Rh/Zr-beta	2	29	100	86 (90)	3	8	3	0	0	86 (77)
6	5 % Rh/Zr-beta	2	22	100	82 (91)	4	12	2	0	0	82 (75)
7	Zr-beta–3 % Ni	3	24	56	< 0.1	3	0	97	0	0	< 0.05
8	Zr-beta–3 % Ni	3	192	100	56 (96)	4	5	35	0	0	56 (54)
9	Zr-beta–15 % Ni	3	3	100	78 (94)	7	15	0	0	0	78 (73)
10	Zr-beta–15 % Ni	2	5	100	92 (94)	3	5	0	0	0	92 (86)
11	Zr-beta–15 % Ni	1	8	100	93 (94)	2	4	1	0	0	93 (87)
12	Zr-beta–15 % Ni	0.2-2	8	100	95 (94)	1	4	0	0	0	95 (89)
13	Zr-beta–2 % Pd (1:1)	2	20	100	58 (94)	0	6	1	0	35	58 (54)
14	Zr-beta–2 % Pd (4:1)	2	20	100	62 (94)	0	5	3	0	30	62 (58)
15	Zr-beta–5 % Pd/C (4:1)	0.2-2	40	100	72 (94)	0	3	3	0	22	72 (68)

[a] Reaction conditions: citral (9.9 mmol), *tert*-butanol (50 mL), catalyst (0.15 g; 0.3 g for dual catalyst system except for Pd systems), 80 °C. X = conversion.

15 wt % Ni/Zr-beta than with 10 wt % Ni/Zr-beta. Over the 15 wt % Ni/Zr-beta, about 75 % of the menthols were formed after 8 h, compared with only 51 % over 10 wt % Ni/Zr-beta. These results show that as the rate of the hydrogenation of **8** to menthols is limiting, a higher nickel loading is helpful in accelerating the reaction. The yield of menthols was similar in both cases, 87–89 %, of which 92–94 % was **9a**. The high diastereoselectivity shows that despite impregnation with a high nickel loading, Zr-beta still contains sufficient intraporous zirconium Lewis acid sites for the stereoselective cyclisation of **2**. However, the final concentrations of **5** and **6** were 4 and 7 %, respectively, compared with the combined total of 4 % obtained in the hydrogenation of (±)-**2**.[18] The higher concentration of byproducts is due to the introduction of hydrogen from the start of the reaction, so that besides the formation of **2**, other competing hydrogenation reactions on citral can also occur (Scheme 1). The rates of these reactions are further enhanced by the high nickel concentration of the catalysts.

Besides the wet impregnation method, deposition–precipitation was also used to deposit nickel on Zr-beta. As confirmed by TEM measurements, the slow rise in pH led to a finer dispersion of the metal than that achieved by wet impregnation. Over this catalyst (Figure 4b), citral was completely converted after 6 h. This is similar to that observed for the catalyst prepared by wet impregnation. However, the concentration of (±)-**2** was higher than that formed over the 15 wt % Ni/Zr-beta prepared by wet impregnation, with a maximum of 25 % compared with 16 % for the catalyst prepared by wet impregnation. This shows that the subsequent reactions on (±)-**2** are hindered. In particular, the rate of the cyclisation step to **8** is decreased, so that the yield of menthols was only 44 %. Instead, a substantial amount of (±)-**2** was hydrogenated to **5** and **6**, with high yields of 35 and 9 %, respectively. The activity results can be correlated to the loss of micropore volume, as observed by nitrogen porosimetry. The use of urea to slowly precipitate out the nickel results in an alkaline medium, which degrades the silica framework of Zr-beta and forms rolled-up sheets of silica "whiskers". The destruction of these well-formed zeolitic pores resulted in Zr-beta with a lower activity and diastereoselectivity for the cyclisation reaction. Compound **9a** was formed with only 78 % selectivity (Table 2, entry 3). Hence, hydrogenation becomes a major route for the transformation of **2** over Ni/Zr-beta-HDP. This is further aided by the small metal particles formed on the catalyst.

Bifunctional Rh/Zr-beta catalyst: For comparison, 0.5, 2 and 5 wt % Rh/Zr-beta samples were tested for the hydrogenation of citral under a pressure of 2 MPa (Figure 5). The rate of reaction over 0.5 wt % Rh/Zr-beta was low. After 24 h, only about 65 % citral was converted. Although the yield of **8** was high, only a small amount, 2 %, of menthols **9a–c** was formed due to the slow hydrogenation of **8**. Increasing the rhodium loading to 2 wt % led to a faster reaction and citral was completely converted after 15 h. An 86 % yield of menthols (with 90 % diastereoselectivity for (±)-menthol **9a**) was obtained after 29 h (Table 2, entry 5). Compounds **5** and **6** formed 11 % of the final products and the remainder was **8**. Further increase of the rhodium loading to 5 wt % resulted in an even higher rate of reaction, and (±)-**2**, **8** and menthols were formed in rapid succession. However, the yield of menthols after 22 h was somewhat lower, 82 %, of which 91 % was the desired isomer **9a**. At this loading, more **5** and **6** (total 16 %) were

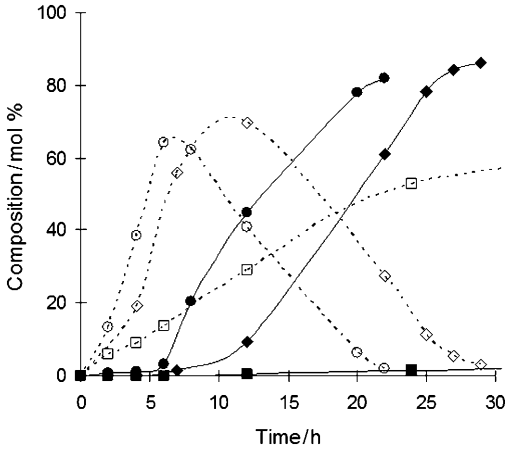

Figure 5. Yield of **8** (open symbols) and menthols (closed symbols) over bifunctional Rh/Zr-beta catalysts with different Rh loadings. (□■) 0.5 wt % (◇◆) 2 wt % and (○●) 5 wt % Rh.

formed. The trend shows that a further increase in rhodium loading to accelerate the rate of hydrogenation is not advantageous as the selectivity towards menthols will be reduced. As with the Ni/Zr-beta catalysts, the hydrogenation of **8** to menthols is slower than that of citral to **2**.

Dual catalyst system of Zr-beta–Ni/MCM-41: In addition to the bifunctional catalyst, dual catalytic systems of Zr-beta and Ni/MCM-41 were also tested for the hydrogenation of citral. This has the advantage that each catalyst can be separately synthesised under conditions best suited to optimise its performance and also variation in the relative proportion of the catalysts can be easily achieved. However, unlike the bifunctional catalyst, the active sites for hydrogenation and cyclisation are on different catalysts and the intermediate molecules must diffuse to and from these sites to form menthol. If **2** is strongly adsorbed on the metal catalyst, then it could undergo hydrogenation to open-chain byproducts, thus lowering the overall selectivity.

Effect of nickel loading: A 1:1 (wt/wt) mixture of 3 wt% Ni/MCM-41 with Zr-beta was tested for catalytic activity at a hydrogen pressure of 3 MPa (Table 2, entries 7 and 8). The low nickel loading was used because the MCM-41 support has a high surface area that should result in a high metal dispersion. Indeed the crystallite size was found to be around 3 nm compared with 27 and 33 nm for 10 wt% Ni/Zr-beta and 15 wt% Ni/Zr-beta, respectively. However, the reaction was very slow and after one day only 56% of the citral was converted. No (±)-**2** was detected because once it formed it immediately cyclised to **8** over Zr-beta. The competing hydrogenation of (±)-**2** to **5** and **6** gave only 3 and 6% of these products, respectively. Their presence became detectable after 2 d when the concentration of citral had dropped to less than 20%. In comparison, the concentration of **8** reached a maximum of 80% after 4 d. The high concentration of **8** in the reaction mixture shows that the 3 wt% Ni/MCM-41 catalyst was not able to catalyse the hydrogenation to menthols at an adequate rate. The yield of menthols was less than 1% after 2 d and slowly increased after almost all of the citral had been converted. However, even after 8 d, compounds **8** were still present in the reaction mixture. The yield of menthols was 56% with a very high diastereoselectivity for **9a** of 96%. The selectivity for byproducts, **5** and **6**, were 4 and 5%, respectively.

To increase the reaction rate, the nickel loading on MCM-41 was increased to 15 wt%. After only 0.5 h at a hydrogen pressure of 3 MPa, the conversion of citral reached 82%. Compound (±)-**2** could be detected after short reaction times, but rapidly cyclised to **8a–c** so that its concentration was low. The concentration of **8** reached a maximum of 29% after 0.5 h and decreased to <2% after 1.5 h (Figure 6). Products **9a–c** were already formed after 0.5 h. After 1.5 h, the conversion of citral was 100% and the entire cascade reaction was completed within 3 h. However, the yield of **9a–c** was only 78%, with the remainder being byproducts **5** and **6**. Hence, the higher nickel loading accelerated the rate of transformation from citral to menthols, but it also increased the rate of competing hydrogenation reactions on citral and **2**, resulting in a lower yield of menthols.

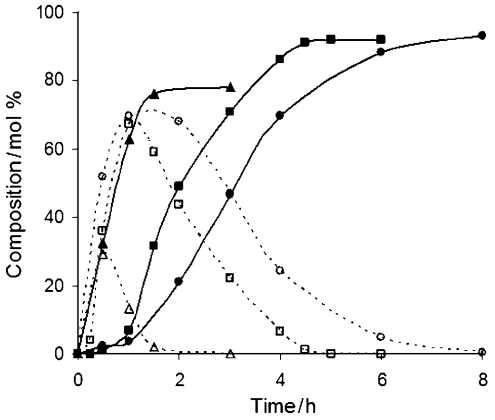

Figure 6. Effect of H_2 pressure on yield of **8** (open symbols) and menthols (closed symbols) over Zr-beta–15 wt% Ni/MCM-41. Pressure: 1 (○●), 2 (□■) and 3 (△▲) MPa.

The diastereoselectivity for the desired product **9a** was similar to that found on Zr-beta, 94%. Hence, it can be inferred that the MCM-41 support did not contribute significantly to the cyclisation reaction. Instead, the bulk (if not all) cyclisation was catalysed within the pore channels of Zr-beta. Compound **2**, formed in the initial hydrogenation over Ni/MCM-41, desorbs and diffuses into the microporous channels of Zr-beta, where it encounters the zirconium active sites for the cyclisation to **8**. Diastereomer **8a** is formed with high selectivity and thereafter, it must desorb and diffuse out of the micropore channels to reach the metal sites on Ni/MCM-41 for the final hydrogenation to menthol.

Effect of H_2 pressure: The reaction was carried out at lower pressures of 1 and 2 MPa in an effort to minimise the formation of byproducts (Figure 6). The rate of citral conversion was slightly decreased at these pressures. For instance, under a hydrogen pressure of 2 MPa, 66% of the citral was converted after 0.5 h and the conversion reached 100% after 2 h. The concentration of **8** was higher at lower pressures. After 1–1.5 h, the concentration of **8** reached a maximum of 68–69% and decreased slowly thereafter. At intermediate times, some **4** and 3,7-dimethyl-2-octenal (**7**) were observed, but their concentrations decreased after longer reaction times due to further hydrogenation.

Depending on the pressure, menthols **9a–c** were formed after an induction time and their rate of formation increased rapidly after 1 h. At 1 MPa, compounds **8** were converted to menthols after 8 h, whereas at 2 MPa, a shorter time of 5 h was required. Under these conditions of lower hydrogen pressure, the yield of menthols was higher (92–93%) than at 3 MPa. The diastereoselectivity for (±)-menthol **9a** was unaffected and remained at around 94%. The total concentration of the byproducts (**5** and **6**) was only 7–8%, compared

with 22% at 3 MPa. The results show that a lower pressure led to a higher yield of menthols, but the reaction took a longer time for completion. The rate of initial citral conversion shows a square-root dependence on the hydrogen pressure, in the range of 0.5 to 5.5 MPa (Figure 7). This is consistent with a simple Langmuir–Hinshelwood model with dissociative adsorption of hydrogen on the nickel sites.

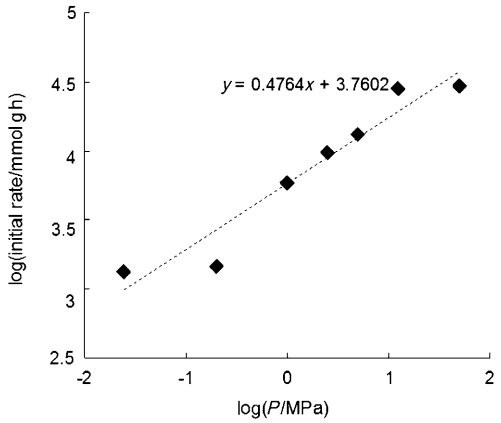

Figure 7. Dependence of citral conversion on hydrogen pressure over Zr-beta–15 wt% Ni/MCM-41.

To further improve the yield of menthols without needing long reaction times, a pressure ramp was applied. The initial pressure was kept low to minimise competing hydrogenation reactions on citral and **2**. After all **2** had been converted, the pressure was raised to facilitate the rate of hydrogenation. Studies into the optimum initial pressures showed that even at 0.2 MPa, the initial hydrogenation of citral was fast with about 60% conversion after 1 h (Figure 8). The reaction was highly selective because more than 96% of the citral had been hydrogenated to **2**, the bulk of which then cyclised to **8** over Zr-beta. After 4 h, when complete conversion of citral

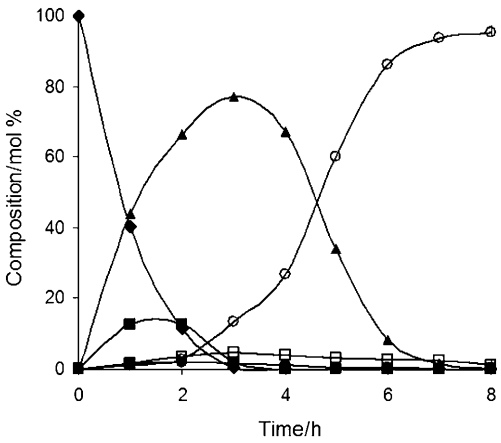

Figure 8. Hydrogenation of citral over Zr-beta–15 wt% Ni/MCM-41 with H_2 pressure ramping from 0.2 to 2 MPa. (◆) Citral (■), **2** (▲), **8** (○) menthols, (□) **5**, and (●) **6**. Reaction conditions: citral (9.9 mmol) *tert*-butanol (50 mL), catalyst (0.3 g), 80 °C.

and **2** had been reached, the selectivity for byproducts, **5** and **6**, remained below 5%. The reaction mixture consisted of 95% **8** and menthols in a ratio of 68:27. Thereafter, the hydrogen pressure could be increased to 2 MPa without affecting the overall selectivity of the cascade reaction. As the hydrogenation of **8** to menthols is slow, the higher pressure helped to increase the rate of this step. The final yield of menthols obtained after 8 h was 95%, of which 94% was (±)-**9a** (Table 2, entry 12).

Reuse of catalysts: A scale up of the experiment was carried out with citral (20 mmol) and the dual catalytic system of Zr-beta–15 wt% Ni/MCM-41. On completion of the reaction, the catalysts were centrifuged from the reaction products and the solvent removed by rotary evaporation. The isolated yield of menthols was 91%. The diastereoselectivity for (±)-menthol in the isolated product was 94%, which is comparable to that obtained over $ZnBr_2$ in the industrial Takasago process for menthol production.[13,23] In many of the runs, catalysts were reused rather than using fresh catalyst. The variation in yield of menthols is within ±4%, similar to that for the fresh catalysts.

Catalytic activity of Zr-beta–Pd/MCM-41: Despite its high activity, the hydrogenation of citral over supported Pd catalysts resulted in the formation of substantial amounts of 3,7-dimethyloctanal (**3**) as a byproduct.[2,3] A bifunctional 1 wt% Pd/HBEA (HBEA = zeolite beta, Si/Al 25) catalyst gave a yield of 26% for **3** and only a yield of 22% for menthols with a diastereoselectivity for **9a** of 47%.[20] Studies of the hydrogen uptake profile have shown that the C=C bond conjugated to the carbonyl group in citral was reduced at the highest rate, followed by the isolated C=C bond and finally the C=O bond.[2] The initial selectivity for **2** is high, >80%. If this molecule could be channelled away to form **8** instead of being hydrogenated to **3**, it would be possible to improve the selectivity for menthols. Because Zr-beta has a high activity for cyclisation of **2**, we used it together with 2 wt% Pd/MCM-41 as a dual catalytic system. A 1:1 mixture of 2 wt% Pd/MCM-41 and Zr-beta catalyst was first tested for citral hydrogenation. Despite the high selectivity of palladium for the formation of **2**, only about 58% yield of menthols was obtained after 20 h (Table 2, entry 13,). Instead, a substantial portion of the **2** was hydrogenated to **3**. This agrees with previous observations of the high propensity of palladium for C=C bond hydrogenation.[2,3] In an attempt to reduce the formation of **3**, the relative amount of Zr-beta to the Pd catalyst was increased to 4:1 (keeping the total catalyst weight constant) to provide more active sites for the cyclisation reaction. The yield of menthols improved to 62% (Table 2, entry 14,). As the rate of hydrogenation of **8** to menthols was decreased due to the smaller amount of Pd/MCM-41, the commercial catalyst 5% Pd/C (Degussa) was used instead. The weight ratio of Zr-beta to the Pd catalyst was kept at 4:1 and the reaction was conducted by using a pressure ramp. Although the initial pressure was kept at 0.2 MPa, the consecutive reaction of **2** to **3** was very fast and

by the time all **2** had been converted, the selectivity for this side product was already 22%. The final yield of menthols was 72%. Although this does not reach the 95% yield obtained with the Zr-beta–Ni/MCM-41 system, these results show that it is possible to optimise a reaction with a dual catalyst system because of the ease in adjusting the relative amounts of the components.

Conclusions

The cascade transformation of citral to menthols occurs with high selectivity when Zr-beta is used as a catalyst. With a Ni loading of 10 and 15 wt%, the total yield of menthols was 88%, with a diastereoselectivity for (±)-menthol of 94%. Modification of the catalyst at the nanoscale is essential for high catalytic activity. Whereas smaller metal crystallites were obtained by the deposition–precipitation method than wet impregnation, the urea used in this preparation destroyed the zeolitic structure. As a consequence, the yield of menthols was decreased in favour of open-chain **5** and **6**. A 2 wt% Rh/Zr-beta catalyst also exhibited good activity with an 86% yield of menthols, although the hydrogenation of **8** to menthols in the final cascade step was slower than with Ni/Zr-beta. A higher loading of 5 wt% Rh increased the rate of hydrogenation, but more **5** and **6** were also formed.

A dual catalytic system of Zr-beta and 15 wt% Ni on MCM-41 gave a high menthol yield of 95% when used together with hydrogen pressure ramping from 0.2 to 2 MPa. The 94% diastereoselectivity for (±)-menthol shows that cyclisation of **2** occurs over active sites on Zr-beta. Hence, the use of Zr-beta in the cascade transformation of citral constitutes a green route to menthols, given the ease of catalyst separation from the reaction medium, minimal loss of activity in subsequent batch cycles and excellent product yield with very high diastereoselectivity.

Experimental Section

Preparation and characterisation of Zr-beta and MCM-41-supported metal catalysts: The syntheses and characterisation of the catalysts have previously been described.[18b,24] The metals were deposited on the supports by wet impregnation at room temperature. Besides incipient wetness impregnation, the homogeneous deposition–precipitation method[25] was also used to prepare a 15 wt% Ni/Zr-beta-HDP sample. Zr-beta (~0.85 g) was immersed in an aqueous solution of $Ni(NO_3)_2$ (0.74 g in 150 mL) and the pH was adjusted to pH 2 with nitric acid. The suspension was heated to 90°C with stirring before an aqueous solution of urea (0.4 g in 10 mL) was added to effect precipitation. After stirring for 18 h, the suspension was cooled to room temperature, filtered, washed, dried at 100°C and calcined at 500°C for 4 h. Prior to catalytic testing, the supported Pd and Ni catalysts were reduced for 2 h in a flow of hydrogen at 150 and at 450°C, respectively, whereas the Rh catalysts were reduced at 300°C for 4 h. The sample was cooled to room temperature in helium, before it was transferred to the autoclave for reaction. No further in situ reduction was carried out in the autoclave.

Catalyst characterisation: The crystal phase of the samples was determined by powder X-ray diffraction by using a Siemens D5005 diffractometer equipped with a Cu anode and variable primary and secondary beam slits. A step size of 0.02° and a dwell time of 1 s were used for the measurements. A step size of 0.004° was used for determining the crystallite size of the deposited metal crystallites. The adsorption–desorption isotherms for the solid samples were measured on a Micromeritics Tristar porosimeter. The samples were degassed under a flow of nitrogen at 300°C for 4 h prior to measurement. TEM measurements were performed with a JEOL JEM 3010 HRTEM microscope operated at 300 kV. Infrared spectra were recorded on a Biorad Excalibur spectrometer with a resolution of 2 cm^{-1}. The sample (5–8 mg) was pressed into a self-supported wafer and mounted in a Pyrex IR cell with NaCl windows. After evacuation under vacuum (10^{-3} mbar) for 2 h at 300°C, it was cooled to room temperature and a background spectrum was recorded. Pyridine was introduced at 22 mbar for 15 min and the system was evacuated for an hour before measuring the spectrum at room temperature. Further IR measurements were made after evacuation at 100 and 200°C.

Catalytic testing: The hydrogenation of citral (containing a mixture of *cis* and *trans* isomers) was carried out in a Teflon-lined 100 mL autoclave (Berghof) with stirring. The autoclave was charged with citral (1.7 mL, 9.9 mmol), catalyst (0.15 g for Zr-beta-supported metal catalysts and Pd-systems; 0.30 g for other dual catalyst systems, typically a 1:1 mixture), *tert*-butanol (50 mL) as solvent and heated to 80°C before hydrogen was introduced into the head space to a pressure of 1 to 5.5 MPa. Samples were removed at regular intervals and analysed by gas chromatography (Agilent GC 6890 equipped with a HP-5 capillary column and an FID detector). The temperature program used for separation of the products was as follows: 60°C for 2 min, 8°C min^{-1} to 130°C, then 25°C min^{-1} to 200°C. The identity of the products was verified by comparison with the retention times of authentic samples and by GC–MS (Shimadzu GCMS-QP5000, DB5 MS column). Figure S1 in the Supporting Information shows a typical chromatogram obtained on completion of the reaction. Each experiment was repeated at least twice with fresh or regenerated catalysts. The deviation in the yields is in the order of ±4%. The variation in the diastereoselectivity for the various isomeric products is in the order of ±1%. For regeneration, the bifunctional catalyst or dual catalyst system was recovered by centrifugation, washed with *tert*-butanol and calcined at 550°C for 4 h. After reduction at the respective temperature, depending on the metal, the sample was cooled to room temperature in helium and introduced into the autoclave for reuse. Regenerated catalyst/dual catalytic system was reused up to five times. Mass balance was checked by adding *m*-xylene (0.2 mL) as an internal standard. In the pressure ramping experiments, the hydrogen pressure was maintained at 0.2 MPa until all citral was converted and no more **2** was detected before increasing to 2 MPa. A two-fold scale up of the experiment was carried out with citral (20 mmol) and the dual catalyst system of Zr-beta–15 wt% Ni/MCM-41. On completion of the reaction, the catalysts were separated from the reaction products and the solvent was removed by rotary evaporation.

Acknowledgements

The authors would like to thank Mr. Yong Lim Foo for his help in interpretation of the TEM images. Financial support from the National University of Singapore under grant number R-143-000-329-112 is gratefully acknowledged.

[1] T. Kieboom in *Catalysis for Renewables: From Feedstock to Energy Production* (Eds.: G. Centi, R. A. van Santen), Wiley-VCH, Weinheim, **2007**, pp. 273–297.
[2] U. K. Singh, M. A. Vannice, *J. Catal.* **2001**, *199*, 73–84.
[3] a) P. Meric, K. M. K. Yu, A. T. S. Kong, S. C. Tsang, *J. Catal.* **2006**, *237*, 330–336; b) S. Yilmaz, S. Ucar, L. Artok, H. Gulec, *Appl. Catal. A* **2005**, *287*, 261–266; c) P. Gallezot, D. Richard, *Catal. Rev.—Sci. Eng.* **1998**, *40*, 81–126; d) E. Asedegbega-Nieto, A. Guerrero-Ruiz, I. Rodríguez-Ramos, *Carbon* **2006**, *44*, 799–823.
[4] a) F. Delbecq, P. Sautet, *J. Catal.* **1995**, *152*, 217–236; b) F. Delbecq, P. Sautet, *J. Catal.* **1996**, *164*, 152–165.

[5] M. A. Aramendía, V. Borau, C. Jiménez, J. M. Marinas, A. Porras, F. J. Urbano, *J. Catal.* **1997**, *172*, 46–54.
[6] P. Mäki-Arvela, L.-P Tiainen, M. Lindblad, K. Demirkan, N. Kumar, R. Sjöholm, T. Ollonqvist, J. Väyrynen, T. Salmi, D. Y. Murzin, *Appl. Catal. A* **2003**, *241*, 271–288.
[7] J. Aumo, S. Oksanen, J.-Y. Mikkola, T. Salmi, D. Y. Murzin, *Ind. Eng. Chem. Res.* **2005**, *44*, 5285–5290.
[8] J. Aumo, J.-P. Mikkola, J. Bernechea, T. Salmi, D. Murzin, *Int. J. Chem. React. Eng.* **2005**, *3*, A25.
[9] J.-P. Mikkola, P. Virtanen, H. Karhu, T. Salmi, D. Y. Murzin, *Green Chem.* **2006**, *8*, 197–205.
[10] K. Bauer, D. Garbe, H. Surburg in *Ullmann's Encyclopedia of Industrial Chemistry, Vol. A11* (Ed.: W. Gerhertz), VCH, Weinheim, **1988**, pp. 168–170.
[11] G. S. Clark, *Perfum. Flavor.* **2007**, *32*, 38–47.
[12] Y. Nakatani, K. Kawashima, *Synthesis* **1978**, 147–148.
[13] H. Yoji, I. Takeshi, O. Yoshiki (Takasago International Corporation) EP 1 225 163A2, **2002**.
[14] a) P. Kočovský, G. Ahmed, J. Šrogl, A. V. Malkov, J. Steele, *J. Org. Chem.* **1999**, *64*, 2765–2775; b) G. D. Yadav, J. J. Nair, *Langmuir* **2000**, *16*, 4072–4079; c) P. Mäki-Arvela, N. Kumar, V. Nieminen, R. Sjöholm, T. Salmi, D. Y. Murzin, *J. Catal.* **2004**, *225*, 155–169; d) J. Tateiwa, A. Kimura, M. Takasuka, S. Uemura, *J. Chem. Soc. Perkin Trans. 1* **1997**, 2169–2174; e) C. Milone, C. Gangemi, G. Neri, A. Pistone, S. Galvagno, *Appl. Catal. A* **2000**, *199*, 239–244; f) N. Ravasio, N. Poli, R. Psaro, M. Saba, F. Zaccheria, *Top. Catal.* **2000**, *13*, 195–199; A. Ramanathan, M. C. C. Villalobos, C. Kwaternaak, S. Telalovic, U. Hanefeld, *Chem. Eur. J.* **2008**, *14*, 961–972.
[15] a) Y. Zhu, Y. T. Nie, S. Jaenicke, G. K. Chuah, *J. Catal.* **2005**, *229*, 404–413; b) G. K. Chuah, S. H. Liu, S. Jaenicke, L. J. Harrison, *J. Catal.* **2001**, *200*, 352–359.
[16] S. R. Bare, S. D. Kelly, W. Sinkler, J. J. Low, F. S. Modica, S. Valencia, A. Corma, L. T. Nemeth, *J. Am. Chem. Soc.* **2005**, *127*, 12924–12932.
[17] M. Boronat, A. Corma, M. Renz, *J. Phys. Chem. B* **2006**, *110*, 21168–21174.
[18] a) Y. T. Nie, G. K. Chuah, S. Jaenicke, *Chem. Commun.* **2006**, 790–792; b) Y. T. Nie, W. L. Niah, S. Jaenicke, G. K. Chuah, *J. Catal.* **2007**, *248*, 1–10.
[19] G. S. Clark, *Perfum. Flavor.* **1988**, *13*, 37–46.
[20] a) A. F. Trasarti, A. J. Marchi, C. R. Apesteguía, *J. Catal.* **2004**, *224*, 484–488; b) A. F. Trasarti, A. J. Marchi, C. R. Apesteguía, *J. Catal.* **2007**, *247*, 155–165.
[21] P. Mäki-Arvela, N. Kumar, D. Kubička, A. Nasir, T. Heikkilä, V.-P. Lehto, R. Sjöholm, T. Salmi, D. Y. Murzin, *J. Mol. Catal. A* **2005**, *240*, 72–81.
[22] E. P. Parry, *J. Catal.* **1963**, *2*, 371–378.
[23] H. van Bekkum, L. Maat in *Catalysis for Renewables: From Feedstock to Energy Production* (Eds.: G. Centi, R. A. Van Santen), Wiley-VCH, Weinheim, **2007**, pp. 101–118.
[24] a) Y. Zhu, G. K. Chuah, S. Jaenicke, *J. Catal.* **2004**, *227*, 1–10; b) Y. Zhu, G. K. Chuah, S. Jaenicke, *Chem. Commun.* **2003**, 2734–2735.
[25] J. H. Bitter, M. K. van der Lee, A. G. T. Slotboom, A. J. van Dillen, K. P. de Jong, *Catal. Lett.* **2003**, *89*, 139–142.

Received: August 28, 2008
Revised: November 13, 2008
Published online: January 8, 2009

